

Fig. S1: Sample locations. Georeferenced Landsat imagery with labelled sampling locations; C = core, B = bank, P = pit samples.

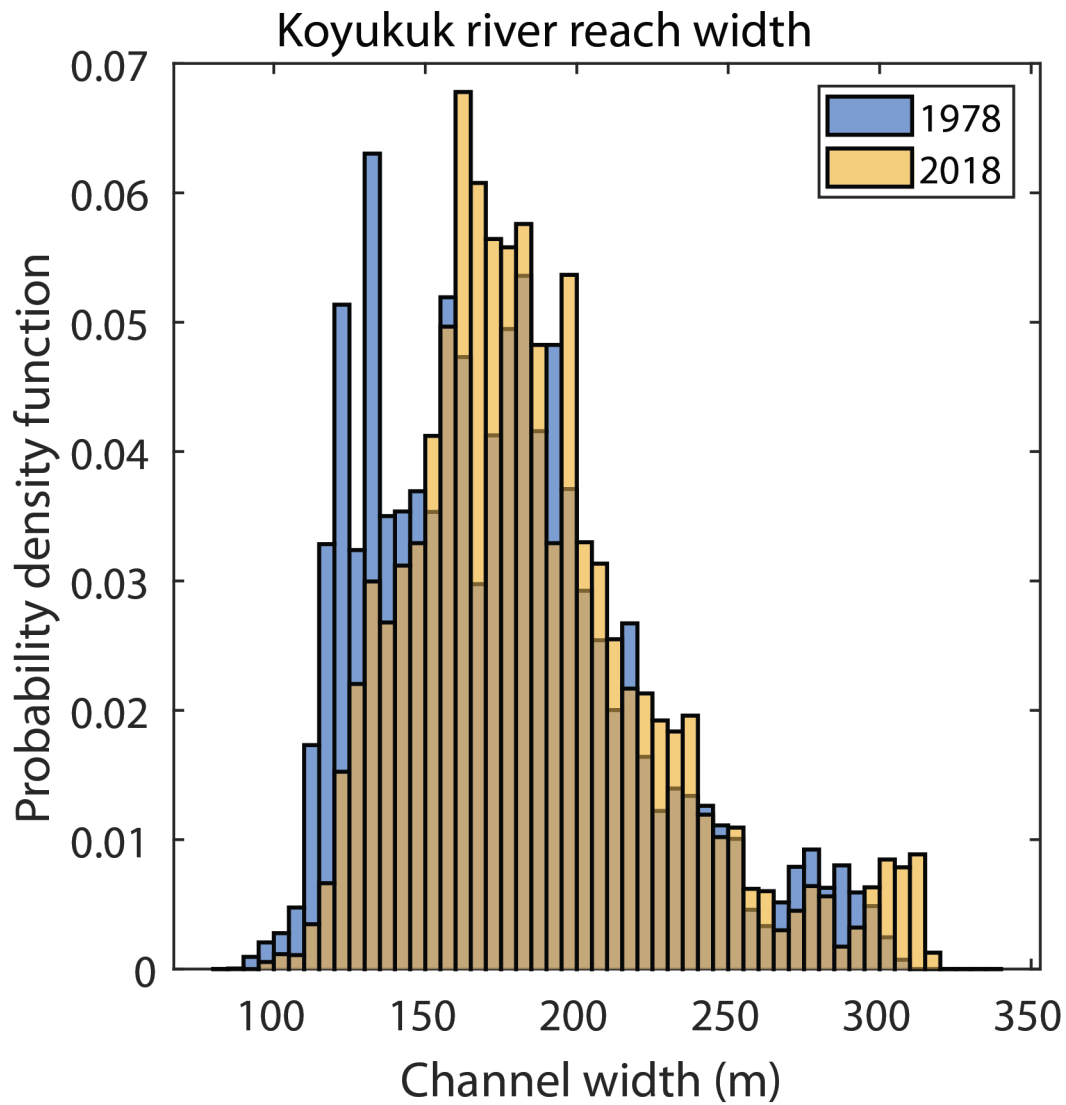
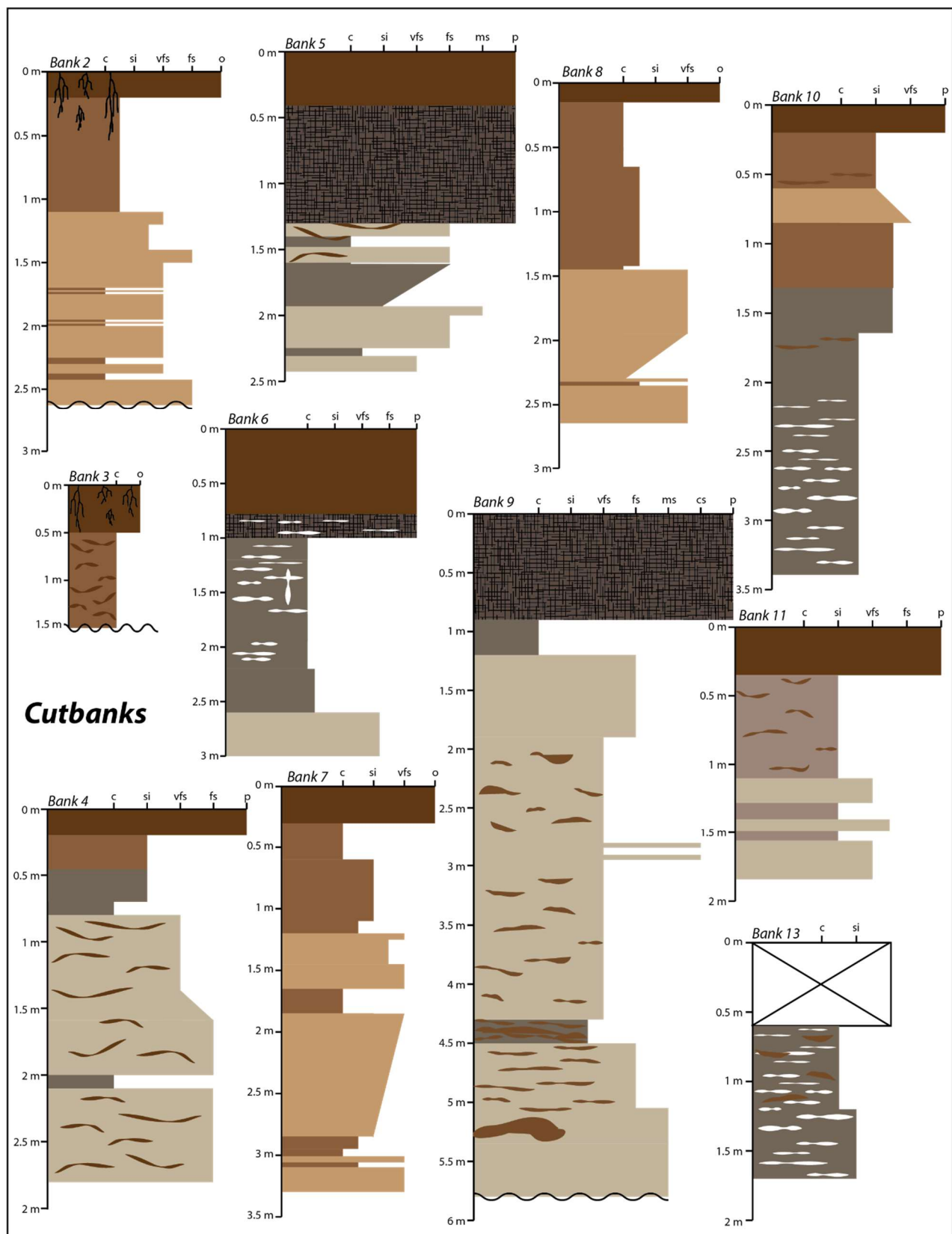


Fig. S2: Koyukuk River width. Probability distribution of width of channel masks generated from Landsat 30 m imagery, with widths calculated at each pixel along the channel centerline for the reach of the Koyukuk River pictured in Fig. S1 (Rowland et al., 2019). The reach maintained a roughly constant channel width over the Landsat record, from 173 ± 43 m (median \pm 1SD) in 1978 to 179 ± 42 m in 2018, supporting our assumption that cutbank erosion and point bar deposition occur at the same rate.



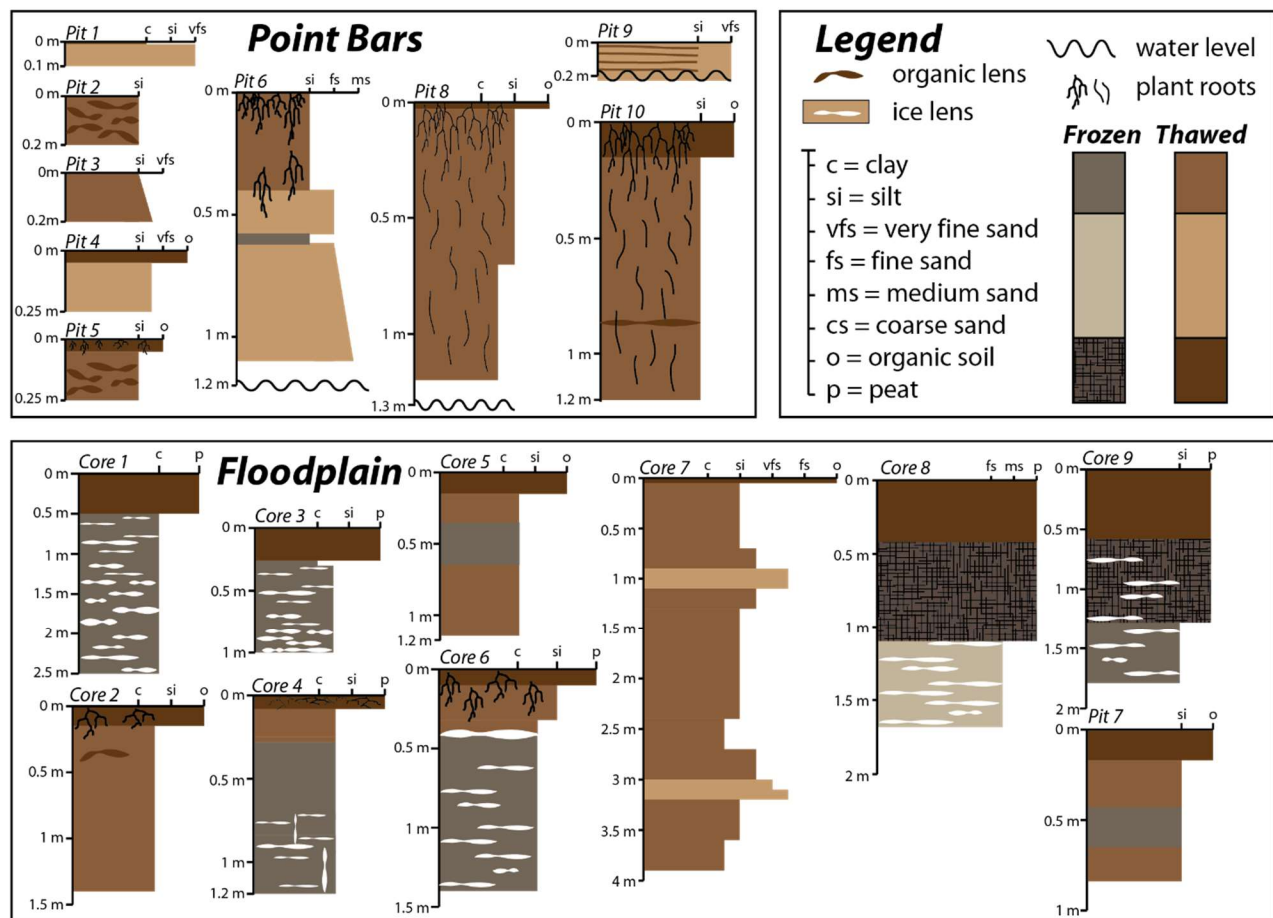


Fig. S3: Measured stratigraphic sections grouped by location on river floodplain. The river channel is eroding its cutbanks and depositing sediment on its point bars, which accrete to form the floodplain as the channel continues to migrate laterally. Note that deposits were generally sandy greater than 2 m depth below the floodplain surface, and that organic horizon thickness at the ground surface varies, though lenses of organic-rich sediment were prevalent meters below the surface. The active layer was shallower in permafrost units containing thick layers of peat, while locations without permafrost contained plant roots extending meters farther below the ground surface and lacked thermoerosional niches. Thicknesses of stratigraphic units were tabulated for each section in Table S4.

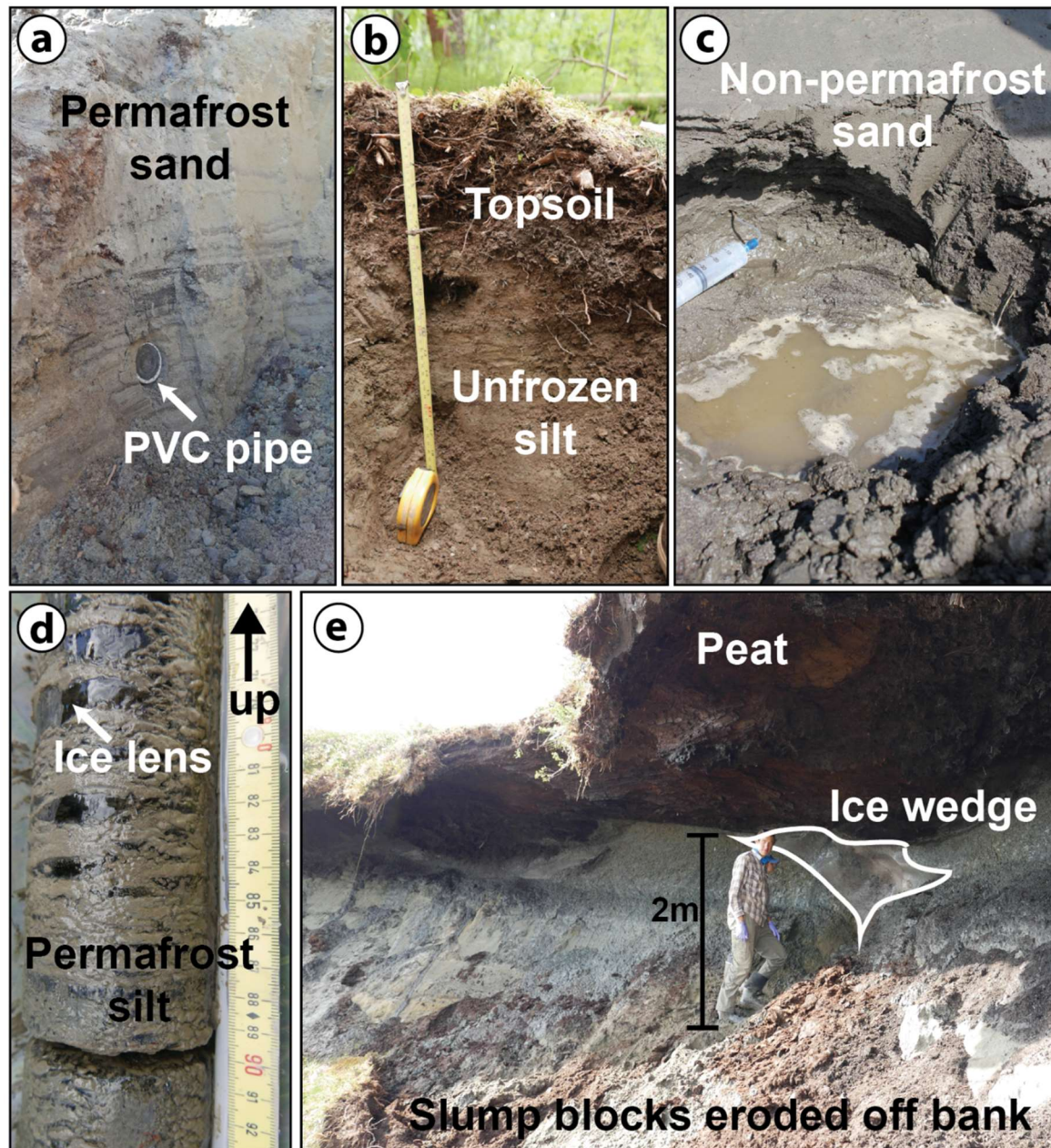
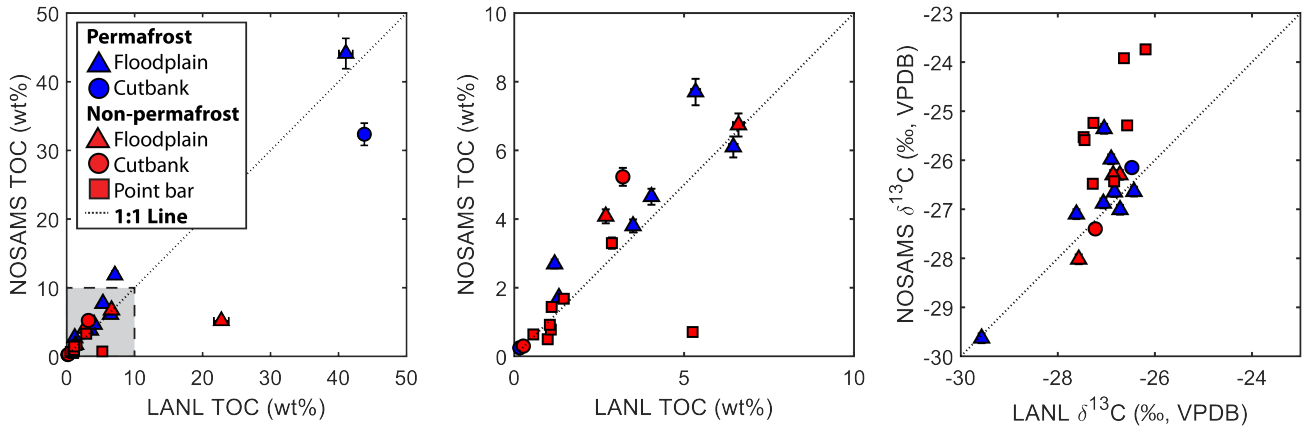


Fig. S4: Field photos of floodplain stratigraphic facies. (a) Permafrost sand in Bank 9 with 2 inch PVC pipe (outer diameter is 6.0 cm) installed in the bank for scale. (b) Pit dug in non-permafrost ground with root-rich topsoil overlying silt at Core 5. (c) Non-permafrost sandy deposits on a point bar beach at Pit 9. (d) Permafrost silt containing ice lenses in Core 4. (e) Overhung cutbank from Bank 9, with a layer of peat overlying an ice wedge surrounded by grey, frozen silt with slump blocks and intraclasts of thawed peat and silt forming a slope that shields the bank.



25 **Fig. S5: Organic carbon measurement comparison.** TOC and OC stable isotopes were measured at both NOSAMS and Los Alamos
 National Lab (LANL), with NOSAMS generally showing a slightly higher TOC and $\delta^{13}\text{C}$. We attribute these differences to
 decarbonation procedures (see Materials and methods). All plots in the main text and supplemental materials use the LANL TOC
 and $\delta^{13}\text{C}$ values with NOSAMS radiocarbon measurements. (a) NOSAMS versus LANL TOC measurements, with error bars
 showing 1SD analytical uncertainty. (b) Zoomed in plot of shaded region in plot (a). (c) NOSAMS versus LANL OC stable isotope
 30 measurements, reported as per mille (‰) relative to VPDB with error bars showing 1SD analytical uncertainty.

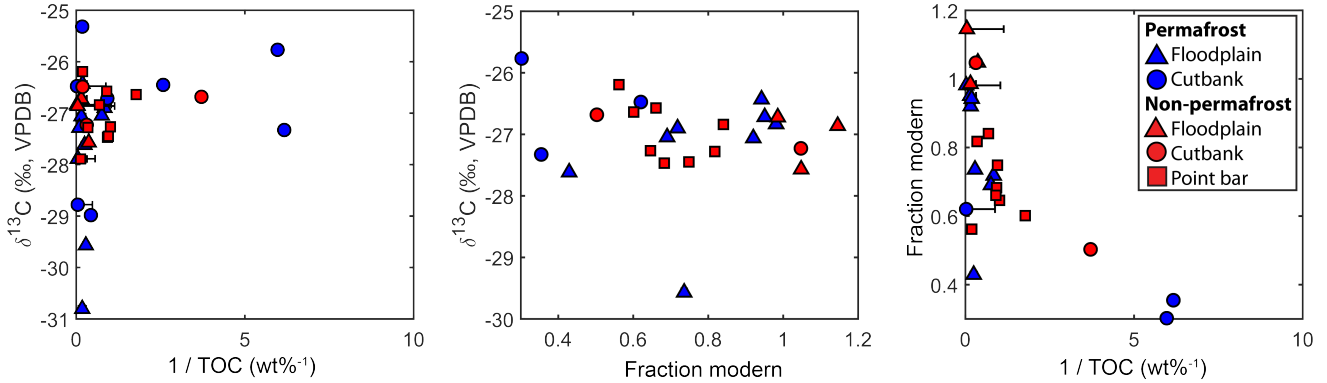
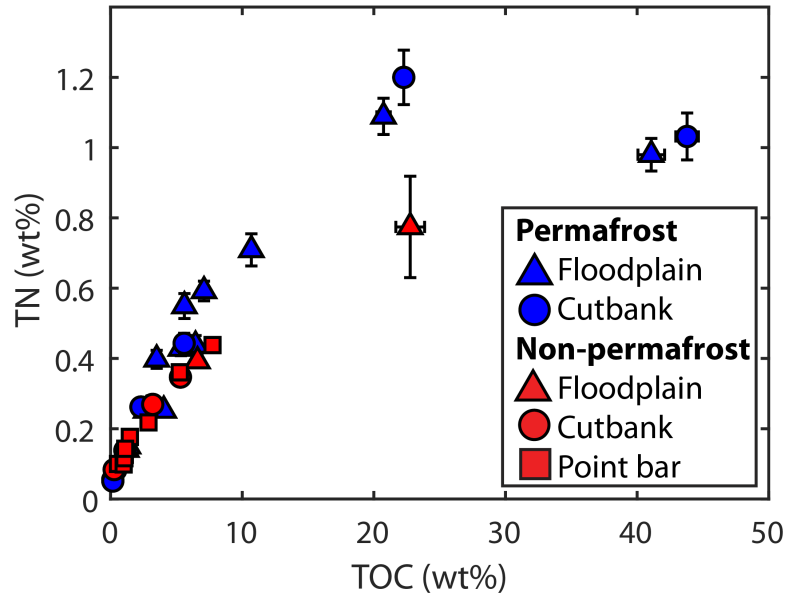


Fig. S6: Sediment OC characteristics. Stable organic carbon isotopes displayed no trends with total organic carbon (TOC) or
 radiocarbon fraction modern (Fm). Sediment $\delta^{13}\text{C}$ values spanned the range previously reported in peat and woody debris (from -
 23.2±0.2 ‰ to -28.6±0.2 ‰) on the Koyukuk River floodplain near its confluence with the Yukon River (O'Donnell et al., 2012).
 35 Stable organic carbon isotope values also incorporated a petrogenic end-member, and kerogen-rich sedimentary rocks in the Brooks
 Range had $\delta^{13}\text{C}$ ranging from -27.23±0.1 ‰ to -30.75±0.1 ‰ (Johnson et al., 2015). Measured $\delta^{13}\text{C}$ values are reported in units of
 per mille (‰) relative to the VPDB, with x and y error bars showing 1SD analytical uncertainty.



40 Fig. S7: Sediment total nitrogen. Total nitrogen (TN) versus total organic carbon (TOC) measured as dry weight % of samples, with error bars showing 1SD analytical uncertainty.

Table S1: Sample site locations and characteristics.

Sample site	Landform	Latitude (°)	Longitude (°)	Frozen ground type
Bank 1	Cutbank	65.78014	-156.43661	Permafrost
Bank 2	Cutbank	65.76493	-156.49031	Non-permafrost
Bank 3	Cutbank	65.76519	-156.48964	Non-permafrost
Bank 4	Cutbank	65.75232	-156.50511	Permafrost
Bank 5	Cutbank	65.75232	-156.50511	Permafrost
Bank 6	Cutbank	65.75232	-156.50511	Permafrost
Bank 7	Cutbank	65.66093	-156.45087	Non-permafrost
Bank 8	Cutbank	65.66126	-156.44711	Non-permafrost
Bank 9	Cutbank	65.70265	-156.40977	Permafrost
Bank 10	Cutbank	65.61942	-156.48534	Permafrost
Bank 11	Cutbank	65.62931	-156.46198	Non-permafrost
Bank 12	Cutbank	65.64022	-156.50949	Non-permafrost
Bank 13	Cutbank	65.87132	-156.26283	Permafrost
Bank 14	Cutbank	65.70153	-156.40353	Permafrost
Core 1	Floodplain	65.78014	-156.43661	Permafrost

Core 2	Floodplain	65.76521	-156.49049	Non-permafrost
Core 3	Floodplain	65.72090	-156.37178	Permafrost
Core 4	Floodplain	65.73519	-156.38866	Permafrost
Core 5	Floodplain	65.67904	-156.61163	Non-permafrost
Core 6	Floodplain	65.67158	-156.58762	Permafrost
Core 7	Point bar	65.66046	-156.43256	Non-permafrost
Core 8	Floodplain	65.72552	-156.20992	Permafrost
Core 9	Floodplain	65.71100	-156.27473	Permafrost
Pit 1	Point bar	65.77817	-156.43370	Non-permafrost
Pit 2	Point bar	65.77764	-156.43364	Non-permafrost
Pit 3	Point bar	65.77688	-156.43394	Non-permafrost
Pit 4	Point bar	65.77636	-156.43342	Non-permafrost
Pit 5	Point bar	65.77483	-156.43354	Non-permafrost
Pit 6	Point bar	65.77756	-156.43381	Non-permafrost
Pit 7	Floodplain	65.72083	-156.37217	Non-permafrost
Pit 8	Point bar	65.65986	-156.43524	Non-permafrost
Pit 9	Point bar	65.65958	-156.43542	Non-permafrost
Pit 10	Point bar	65.66132	-156.43354	Non-permafrost

Table S2: Sample descriptions and results of laboratory analysis. Starred samples have median grain size (D_{50}), TOC, TN, $\delta^{13}C$ and molar TOC/TN ratios previously reported in Douglas et al. (2021).

45 Attached as file TableS2.txt

Table S3: Averaged sediment TOC concentrations and constants used in calculations of bank TOC integrated to channel depth.

	Sand	Silt	Peat	Topsoil
D_{50} (mm)	>0.063	<0.063	N/A	N/A
Water content (wt%)	18.1±6.1	46.6±15.6	87.5±7.4	62.2±1.0
TOC (wt%)	0.94±0.95	3.69±2.25	35.20±12.60	15.25±10.62
TOC (kgC/m³)	7.49±8.27	19.1±14.4	42.7±20.0	55.9±42.2
TOC_{petro} (wt%)	0.108±0.045	0.108±0.045	0.108±0.045	0.108±0.045
TOC_{petro} (kgC/m³)	0.86±0.52	0.56±0.34	0.13±0.07	0.40±0.20
TOC_{bio} (wt%)	0.83±0.95	3.58±2.25	35.09±12.60	15.14±10.62
TOC_{bio} (kgC/m³)	6.63±8.13	18.57±14.29	42.55±20.00	55.52±42.18

Bulk density (kg/m ³)	971±283
Channel Depth (m)	12.4
Migration Rate (m/yr)	0.52

Table S4: Calculation of bank TOC, biospheric, and petrogenic components integrated to channel depth based on measured stratigraphic columns. Note that unmeasured section was assumed to consist of sand based on field observations.

50 Attached as file TableS4.txt

Table S5: Complete grain size distributions measured using laser diffraction tabulated in log-normal bins, with 10th-, 50th- and 90th-percentile grain size reported as D₁₀, D₅₀, and D₉₀.

Attached as file TableS5.txt

55

Table S6: Linear mixing calculations of fraction modern of biospheric OC and fraction of biospheric OC produced *in-situ* (as opposed to being deposited in association with the sediment by the river). End-members for transported OC (Fm of oldest woody debris from a cutbank) and *in situ* produced OC (youngest topsoil *Fm_{bio}*) are italicized.

Sample Name	Sample Type	Biospheric fraction modern (<i>Fm_{bio}</i>)	Fraction <i>in-situ</i> biomass (<i>f_{bio, is}</i>)
KY18-Bank2-10	Cutbank sediment	1.0837±0.0330	0.9272±0.0825
KY18-Bank2-230	Cutbank sediment	0.8398±0.1015	0.6617±0.0906
KY18-Bank9-Peat	Cutbank sediment	0.6217±0.0173	0.4243±0.0355
KY18-Bank9-220	Cutbank sediment	1.0631±0.1776	0.9047±0.1890
KY18-Bank9-350	Cutbank sediment	0.8509±0.1396	0.6737±0.1158
KY18-Core1-22-28	Floodplain sediment	0.9359±0.0265	0.7662±0.0662
KY18-Core1-105-111	Floodplain sediment	0.7593±0.0228	0.5740±0.0489
KY18-Core2-10-12	Floodplain sediment	1.0916±0.0413	0.9357±0.0870
KY18-Core2-35-37	Floodplain sediment	1.0018±0.0354	0.8380±0.0755
KY18-Core3-15-20	Floodplain sediment	0.9653±0.0340	0.7983±0.0714
KY18-Core3-84-89	Floodplain sediment	0.7899±0.0380	0.6074±0.0554
KY18-Core4-16-20	Floodplain sediment	0.9616±0.0342	0.7942±0.0711
KY18-Core4-105-110	Floodplain sediment	0.7521±0.0347	0.5662±0.0508
<i>KY18-Core5-15</i>	<i>Floodplain sediment</i>	<i>1.1507±0.0781</i>	
KY18-Core7-85-95	Point bar sediment	0.7440±0.0551	0.5574±0.0563
KY18-Core7-390-400	Point bar sediment	0.5736±0.0205	0.3719±0.0314
KY18-Core9-33-38	Floodplain sediment	0.9837±0.0344	0.8183±0.0733

KY18-Core9-169-174	Floodplain sediment	0.4409±0.0160	0.2275±0.0190
KY18-Pit1-5	Point bar sediment	0.7253±0.0383	0.5371±0.0491
KY18-Pit2-10	Point bar sediment	0.8494±0.0319	0.6721±0.0595
KY18-Pit4-20	Point bar sediment	0.7588±0.0382	0.5735±0.0524
KY18-Pit5-20	Point bar sediment	0.9077±0.0401	0.7356±0.0679
KY18-Pit6-60	Point bar sediment	0.8343±0.0426	0.6556±0.0614
KY18-Pit8-40	Point bar sediment	0.7323±0.0365	0.5446±0.0493
<i>KY18-Bank14</i>	<i>Cutbank woody debris</i>	<i>0.2319±0.00152</i>	